Electronic supplementary information (ESI) for

β-$LaTeBO_5$ and $RETeBO_5$ (RE = Y, Gd, Tb): Explorations of New Optical Materials in the RE(III)-Te(IV)-B-O System

Peng-Fei Chen [a,b,c], *Chun-Li Hu* [a], *Ming-Zhi Zhang* [a], *Jiang-Gao Mao*[*a, b, c]

a State Key Laboratory of Structural Chemistry, Fujian Institute of Research on the Structure of Matter, Chinese Academy of Sciences, Fuzhou 350002, P. R. China.

b School of Physical Science and Technology, ShanghaiTech University, Shanghai 201210, P. R. China.

c University of Chinese Academy of Sciences, Beijing 100049, China.

* Corresponding Author: mjg@fjirsm.ac.cn

Table of Contents

Section	Title	Page
Table S1	Crystallographic data for β-$LaTeBO_5$ and $RETeBO_5$ (RE= Y, Gd, Tb).	S1
Table S2	Selected Bond distances (Å) and angles (°) for β-$LaTeBO_5$.	S2-S3
Table S3	Selected Bond distances (Å) and angles (°) for $RETeBO_5$ (RE= Y, Gd, Tb).	S4-S5
Table S4	Assignment of the absorption peaks observed in the IR spectrum of β-$LaTeBO_5$ and $RETeBO_5$ (RE = Y, Gd, Tb).	S6
Table S5	The space group, Te-π groups FBB, energy gap and optical properties comparison of containing Te and π-conjugate groups systems.	S7
Figure S1	The photographs of crystals for β-$LaTeBO_5$ and $RETeBO_5$ (RE = Y, Gd, Tb).	S8
Figure S2	Simulated and experimental powder X-ray diffraction patterns of β-$LaTeBO_5$ and $RETeBO_5$ (RE= Y, Gd, Tb).	S9
Figure S3	EDS spectrum of β-$LaTeBO_5$ (a) and $RETeBO_5$ (RE = Y (b), Gd (c), Tb (d)).	S10
Figure S4	The coordination environment of La1 (a) and La2 (b) in β-$LaTeBO_5$.	S11
Figure S5	Plot of lattice constant (which contains the a, b, c and V) for $RETeBO_5$ (RE = Y, Gd, Tb) against the RE^{3+} ionic radius.	S12
Figure S6	TG curves of β-$LaTeBO_5$ and $RETeBO_5$ (RE = Y, Gd, Tb).	S13
Figure S7	Characterizations of β-$LaTeBO_5$ and $RETeBO_5$ (RE = Y, Gd, Tb): (a) IR spectrum; (b) UV-vis-NIR diffuse reflectance spectrum; (c) converted F(R)-versus-Energy plot.	S14
Figure S8	The positive and negative rotation of compensatory, and the thickness of β-$LaTeBO_5$ (a), $YTeBO_5$ (b) and $GdTeBO_5$ (c).	S15
Figure S9	The calculated band structure of β-$LaTeBO_5$ (a) and $RETeBO_5$ (RE = Y(b), Gd(c))	S16
Figure S10	Total and partial density of states of β-$LaTeBO_5$ (a) and $RETeBO_5$ (RE = Y(b), Gd(c)).	S17
Figure S11	Electron density difference maps of $[TeO_3]^{2-}$ units in β-$LaTeBO_5$ along the *b* axis.	S18

Table S1. Crystallographic data for β-$LaTeBO_5$ and $RETeBO_5$ (RE = Y, Gd, Tb).

Formula	$La_2Te_2B_2O_{10}$	$YTeBO_5$	$GdTeBO_5$	$TbTeBO_5$
Formula weight	714.64	307.32	375.66	377.33
Crystal system	Monoclinic	Orthorhombic	Orthorhombic	Orthorhombic
Space group	$P2_1/c$ (No. 14)	*Pbca* (No. 61)	*Pbca* (No. 61)	*Pbca* (No. 61)
T (K)	150.00(2)	297.76(10)	150.01(10)	295.67(10)
a (Å)	16.7501(6)	10.4579(10)	10.5878(5)	10.5343(9)
b (Å)	7.1820(2)	6.5842(7)	6.6574(3)	6.6235(6)
c (Å)	8.3492(3)	11.0918(15)	11.2141(6)	11.1528(11)
β (º)	104.124(3)	90	90	90
V (Å^3)	974.04(6)	763.75(15)	790.45(7)	778.17(12)
Z	4	8	8	8
λ (Mo-Ka) (Å)	0.71073	0.71073	0.71073	0.71073
Dc (g/cm^{-3})	4.873	5.345	6.313	6.441
μ (mm^{-1})	14.561	22.656	23.915	25.423
GOF on F^2	1.068	1.083	1.084	1.113
R_1, wR_2 [$I > 2\sigma(I)$]	0.0191, 0.0376	0.0344, 0.0788	0.0228, 0.0471	0.0220, 0.0509
R_1, wR_2 (all data)	0.0225, 0.0391	0.0391, 0.0827	0.0267, 0.0489	0.0234, 0.0523

$R_1 = \Sigma||F_o| - |F_c||/\Sigma|F_o|$ and $wR_2 = \{\Sigma[w(F_o^2 - F_c^2)^2] / \Sigma[wF_o^2]^2\}^{1/2}$.

Table S2. Selected Bond distances (Å) and angles (°) for β-$LaTeBO_5$.

β-$LaTeBO_5$			
Selected bond distances			
La1–O1$^{\#2}$	2.496(3)	La2–O10$^{\#7}$	2.620(3)
La1–O2$^{\#3}$	2.597(3)	La2–O10$^{\#8}$	2.579(3)
La1–O2$^{\#4}$	2.623(3)	La2–O10$^{\#6}$	2.847(3)
La1–O2$^{\#1}$	2.929(3)	Te1–O1	1.856(3)
La1–O3	2.435(3)	Te1–O2	1.859(3)
La1–O3$^{\#1}$	2.530(3)	Te1–O3	1.863(3)
La1–O4	2.429(3)	Te2–O8	1.863(3)
La1–O4$^{\#2}$	2.616(3)	Te2–O9	1.850(3)
La1–O5$^{\#2}$	2.750(3)	Te2–O10	1.866(3)
La2–O6$^{\#2}$	2.706(3)	B1–O4	1.305(6)
La2–O7	2.446(3)	B1–O5	1.396(6)
La2–O7$^{\#2}$	2.601(3)	B1–O6	1.392(6)
La2–O8$^{\#6}$	2.536(3)	B2–O5$^{\#2}$	1.389(6)
La2–O8	2.446(3)	B2–O6	1.395(6)
La2–O9$^{\#2}$	2.532(3)	B2–O7	1.319(6)
Selected bond angles			
O1$^{\#2}$–La1–O3$^{\#1}$	73.25(11)	O7–La2–O10$^{\#7}$	67.71(10)
O1$^{\#2}$–La1–O2$^{\#1}$	102.50(9)	O7–La2–O10$^{\#8}$	78.20(10)
O1$^{\#2}$–La1–O2$^{\#3}$	125.89(10)	O7$^{\#2}$–La2–O6$^{\#2}$	51.72(9)
O1$^{\#2}$–La1–O2$^{\#4}$	64.96(10)	O7$^{\#2}$–La2–O10$^{\#5}$	62.29(9)
O1$^{\#2}$–La1–O4$^{\#2}$	72.30(11)	O7$^{\#2}$–La2–O10$^{\#7}$	164.98(10)
O1$^{\#2}$–La1–O5$^{\#2}$	77.40(12)	O8–La2–O6$^{\#2}$	79.42(10)
O2$^{\#3}$–La1–O5$^{\#2}$	132.22(10)	O8–La2–O7	74.57(10)
O2$^{\#3}$–La1–O2$^{\#1}$	105.16(10)	O8–La2–O7$^{\#2}$	74.23(10)
O2$^{\#4}$–La1–O2$^{\#1}$	132.58(7)	O8–La2–O8$^{\#5}$	124.31(8)
O2$^{\#4}$–La1–O2$^{\#3}$	61.97(11)	O8–La2–O9$^{\#2}$	144.13(11)
O2$^{\#4}$–La1–O4$^{\#2}$	136.86(10)	O8–La2–O10$^{\#5}$	69.92(9)
O2$^{\#4}$–La1–O5$^{\#2}$	111.69(10)	O8–La2–O10$^{\#7}$	91.86(10)
O3–La1–O1$^{\#2}$	144.96(11)	O8–La2–O10$^{\#8}$	147.44(9)
O3–La1–O2$^{\#1}$	70.19(9)	O8$^{\#5}$–La2–O6$^{\#2}$	139.84(10)
O3–La1–O2$^{\#3}$	88.50(9)	O8$^{\#5}$–La2–O7$^{\#2}$	100.01(9)

O3–La1–O2$^{\#4}$	145.02(9)	O8$^{\#5}$–La2–O10$^{\#5}$	59.66(9)
O3–La1–O3$^{\#1}$	122.96(8)	O8$^{\#5}$–La2–O10$^{\#7}$	82.99(9)
O3–La1–O4$^{\#2}$	74.38(10)	O8$^{\#5}$–La2–O10$^{\#8}$	73.21(10)
O3–La1–O5$^{\#2}$	73.35(10)	O9$^{\#2}$–La2–O6$^{\#2}$	71.50(11)
O3$^{\#1}$–La1–O2$^{\#1}$	58.14(9)	O9$^{\#2}$–La2–O7$^{\#2}$	71.39(10)
O3$^{\#1}$–La1–O2$^{\#3}$	83.43(10)	O9$^{\#2}$–La2–O8$^{\#5}$	72.34(11)
O3$^{\#1}$–La1–O2$^{\#4}$	74.67(10)	O9$^{\#2}$–La2–O10$^{\#5}$	102.03(9)
O3$^{\#1}$–La1–O4$^{\#2}$	98.94(9)	O9$^{\#2}$–La2–O10$^{\#7}$	123.24(10)
O3$^{\#1}$–La1–O5$^{\#2}$	143.44(9)	O9$^{\#2}$–La2–O10$^{\#8}$	63.05(10)
O4–La1–O1$^{\#2}$	107.46(11)	O10$^{\#7}$–La2–O6$^{\#2}$	132.30(9)
O4–La1–O2$^{\#1}$	146.36(10)	O10$^{\#7}$–La2–O10$^{\#5}$	108.04(10)
O4–La1–O2$^{\#3}$	68.80(10)	O10$^{\#8}$–La2–O6$^{\#2}$	104.69(10)
O4–La1–O2$^{\#4}$	75.49(10)	O10$^{\#8}$–La2–O7$^{\#2}$	133.91(10)
O4–La1–O3	76.50(10)	O10$^{\#8}$–La2–O10$^{\#5}$	132.81(7)
O4–La1–O4$^{\#2}$	113.61(11)	O10$^{\#8}$–La2–O10$^{\#7}$	61.09(11)
O4–La1–O3$^{\#1}$	146.26(10)	O1–Te1–O2	96.09(15)
O4–La1–O5$^{\#2}$	64.14(9)	O1–Te1–O3	103.03(14)
O4$^{\#2}$–La1–O2$^{\#1}$	61.77(9)	O2–Te1–O3	91.90(14)
O4$^{\#2}$–La1–O2$^{\#3}$	161.05(10)	O8–Te2–O10	92.39(13)
O4$^{\#2}$–La1–O5$^{\#2}$	50.78(9)	O9–Te2–O8	102.79(14)
O5$^{\#2}$–La1–O2$^{\#1}$	109.11(9)	O9–Te2–O10	94.33(14)
O6$^{\#2}$–La2–O10$^{\#5}$	112.35(9)	O4–B1–O5	117.1(4)
O7–La2–O6$^{\#2}$	64.75(9)	O4–B1–O6	128.4(4)
O7–La2–O7$^{\#2}$	112.60(11)	O6–B1–O5	114.4(4)
O7–La2–O8$^{\#5}$	146.37(10)	O5$^{\#2}$–B2–O6	114.8(4)
O7–La2–O9$^{\#2}$	109.74(10)	O7–B2–O5$^{\#2}$	128.0(4)
O7–La2–O10$^{\#5}$	144.13(10)	O7–B2–O6	117.2(4)

Symmetry transformations used to generate equivalent atoms:

#1: -X, 0.5+Y, 0.5-Z; #2: +X, 0.5-Y, -0.5+Z; #3: -X, -Y, 1-Z; #4: +X, 1+Y, +Z; #5: 1-X, -0.5+Y, 0.5-Z; #6: 1-X, 0.5+Y, 0.5-Z; #7: 1-X, 1-Y, 1-Z; #8: +X, -1+Y, +Z;

Table S3. Selected Bond distances (Å) and angles (°) for $RETeBO_5$ (RE = Y, Gd, Tb).

$RETeBO_5$ (RE= Y, Gd, Tb)	**Y**	**Gd**	**Tb**
Selected bond distances			
RE1–O1$^{\#4}$	2.495(5)	2.501(4)	2.493(4)
RE1–O1$^{\#5}$	2.307(4)	2.357(4)	2.335(4)
RE1–O2$^{\#4}$	2.391(4)	2.441(4)	2.427(4)
RE1–O3	2.317(4)	2.365(4)	2.350(4)
RE1–O3$^{\#2}$	2.336(4)	2.371(4)	2.356(4)
RE1–O4	2.393(4)	2.422(4)	2.410(4)
RE1–O4$^{\#3}$	2.341(4)	2.387(4)	2.365(4)
RE1–O5$^{\#2}$	2.452(5)	2.495(4)	2.473(5)
Te1–O2	2.089(4)	2.074(4)	2.070(4)
Te1–O4	1.868(5)	1.874(5)	1.873(4)
Te1–O5	1.900(5)	1.906(4)	1.901(5)
Te1–O5$^{\#6}$	2.164(5)	2.181(5)	2.174(4)
B1–O1	1.356(9)	1.356(8)	1.343(7)
B1–O2	1.388(9)	1.419(8)	1.406(8)
B1–O3	1.364(8)	1.360(8)	1.366(7)
Selected bond angles			
O1$^{\#5}$–RE1–O1$^{\#4}$	140.03(7)	139.84(6)	139.89(5)
O1$^{\#5}$–RE1–O2$^{\#4}$	150.56(15)	149.87(16)	150.18(15)
O1$^{\#5}$–RE1–O3	79.16(16)	79.13(16)	79.12(14)
O1$^{\#5}$–RE1–O3$^{\#1}$	92.89(15)	92.40(15)	92.31(14)
O1$^{\#5}$–RE1–O4	85.44(17)	85.50(16)	85.97(15)
O1$^{\#5}$–RE1–O4$^{\#3}$	92.95(18)	93.23(15)	93.00(15)
O1$^{\#5}$–RE1–O5$^{\#1}$	70.19(17)	69.47(15)	69.61(15)
O2$^{\#4}$–RE1–O1$^{\#4}$	56.66(15)	56.71(14)	56.63(13)
O2$^{\#4}$–RE1–O4	71.45(16)	116.60(14)	116.60(14)
O2$^{\#4}$–RE1–O5$^{\#1}$	116.57(16)	84.65(14)	85.05(14)
O3–RE1–O1$^{\#4}$	85.23(16)	78.37(15)	78.57(14)
O3–RE1–O2$^{\#4}$	79.10(15)	138.74(5)	138.71(4)
O3–RE1–O3$^{\#1}$	138.51(6)	79.82(15)	79.84(15)
O3–RE1–O4	80.14(17)	147.25(15)	146.99(15)

O3–RE1–O4$^{\#3}$	146.81(17)	63.53(14)	63.90(14)
O3–RE1–O5$^{\#1}$	64.09(16)	76.20(15)	75.88(13)
O3$^{\#1}$–RE1–O1$^{\#4}$	75.08(15)	117.72(16)	117.50(14)
O3$^{\#1}$–RE1–O2$^{\#4}$	116.53(15)	140.25(15)	140.32(14)
O3$^{\#1}$–RE1–O4	140.31(17)	72.73(15)	72.95(15)
O3$^{\#1}$–RE1–O4$^{\#3}$	73.46(17)	75.62(15)	75.20(15)
O3$^{\#1}$–RE1–O5$^{\#1}$	74.85(16)	127.44(15)	127.21(14)
O4–RE1–O1$^{\#4}$	127.86(16)	71.00(15)	70.82(14)
O4–RE1–O5$^{\#1}$	139.42(16)	138.37(15)	138.99(14)
O4$^{\#3}$–RE1–O1$^{\#4}$	118.50(17)	118.60(15)	118.59(15)
O4$^{\#3}$–RE1–O2$^{\#4}$	94.46(16)	94.93(14)	95.02(14)
O4$^{\#3}$–RE1–O4	67.0(2)	67.79(19)	67.58(17)
O4$^{\#3}$–RE1–O5$^{\#1}$	143.07(15)	143.08(15)	142.85(14)
O5$^{\#1}$–RE1–O1$^{\#4}$	69.88(16)	70.40(15)	70.33(14)
O2–Te1–O5$^{\#6}$	164.95(18)	165.17(17)	165.18(17)
O4–Te1–O2	90.19(19)	90.18(19)	90.07(17)
O4–Te1–O5	95.3(2)	96.04(19)	96.02(18)
O4–Te1–O5$^{\#6}$	84.87(19)	84.73(19)	85.08(18)
O5–Te1–O2	89.91(19)	90.66(18)	90.45(18)
O5–Te1–O5$^{\#6}$	76.5(2)	76.1(2)	76.2(2)
O1–B1–O2	115.4(6)	115.5(6)	116.2(5)
O1–B1–O3	125.3(7)	125.5(6)	125.6(6)
O3–B1–O2	118.9(6)	118.8(6)	118.0(5)

Symmetry transformations used to generate equivalent atoms:

#1: 1-X, 0.5+Y, 1.5-Z; #2: 1-X, -0.5+Y, 1.5-Z; #3: 1-X, -Y, 1-Z; #4: 1.5-X, -0.5+Y, +Z; #5: -0.5+X, +Y, 1.5-Z; #6: 1-X, 1-Y, 1-Z; #7: 1.5-X, 0.5+Y, +Z; #8: 0.5+X, +Y, 1.5-Z;

Table S4. Assignment of the absorption peaks observed in the IR spectrum of β-$LaTeBO_5$ and $RETeBO_5$ (RE = Y, Gd, Tb).

Mode description	Absorption peaks (cm^{-1})			
	β-$LaTeBO_5$	$YTeBO_5$	$GdTeBO_5$	$TbTeBO_5$
$\nu_{as}(BO_3)$	1503, 1319, 1170	1328, 1181	1328, 1170	1328, 1174
$\nu_{s}(BO_3)$	916	943	937	935
$\delta(BO_3)$		592	582	586
$\nu_{s, as}(TeO_3)$	688, 445	705, 657, 470	703, 655, 460	703, 653, 462

Table S5. The space group, Te-π groups FBB, energy gap and optical properties comparison of containing Te(IV) and π-conjugate groups systems.

S/N	Compounds	Space Group	Te-π groups FBB	E_g /(eV)	Birefringence	Ref.
Tellurite Borate						
1	$Ca_{13}Te_{4.42}O_{15}(BO_3)_4(OH)_3$	*P*2$_1$/*c*	$[BO_3]^{3-}$, $[TeO_6]^{6-}$, $[TeO_3]^{2-}$	N/A	N/A	1
2	$Rb_3BaTeB_7O_{15}$	*P*2$_1$/*n*	2D $[TeB_7O_{15}]$	4.3	0.035@1064nm	2
3	$K_3BaTeB_7O_{15}$	*P*2$_1$/*n*	2D $[TeB_7O_{15}]$	4.2	0.030@1064nm	3
4	$PbTeB_4O_9$	*P*-1	2D $[B_4TeO_8]$	4.58	0.099@1064nm	4
5	TeB_4O_8	*C*2/*c*	3D $[TeB_4O_8]$	N/A	N/A	5
6	$Te_2B_2O_7$	*Pna*2$_1$	3D $[Te_2B_2O_7]$	4.8	N/A	6
7	α-$LaTeBO_5$	*Pbca*	0D $[Te_2O_4(BO_3)_2]^{6-}$	4.2	0.080@1064nm	7
8	$GdTeBO_5$	*Pbca*	0D $[Te_2O_4(BO_3)_2]^{6-}$	4.42	0.074@546nm	This work
9	$YTeBO_5$	*Pbca*	0D $[Te_2O_4(BO_3)_2]^{6-}$	4.46	0.080@546nm	This work
10	$TbTeBO_5$	*Pbca*	0D $[Te_2O_4(BO_3)_2]^{6-}$	3.74	N/A	This work
11	β-$LaTeBO_5$	*P*2$_1$/*c*	1D $[BO_2]_\infty$, $[TeO_3]^{2-}$	4.08	0.134@546nm	This work
Tellurite Carbonate						
1	$CaTeO_2(CO_3)$	*Pbca*	$[TeO_3]^{2-}$, $[CO_3]^{2-}$	N/A	N/A	8
2	$Rb_2Zn(TeO_3)(CO_3)\cdot H_2O$	*I*2/*c*	$[TeO_3]^{2-}$, $[CO_3]^{2-}$	N/A	N/A	9
3	$LiKTeO_2(CO_3)$	*P*2$_1$/*n*	0D $[Te_2C_2O_{10}]^{4-}$	4.58	0.029@1064nm	10
4	$NaKTeO_2(CO_3)$	*P*2$_1$/*n*	0D $[Te_2C_2O_{10}]^{4-}$	4.27	0.040@1064nm	10
Tellurite Nitrate						
1	$Bi_2Te_2O_6(NO_3)_2(OH)_2(H_2O)$	*P*2$_1$2$_1$2$_1$	$[TeO_3]^{2-}$, $[TeO_6]^{6-}$, $[NO_3]^-$	4	N/A	11
2	$AgTeO_2NO_3$	*Pbcn*	$[TeO_4]^{4-}$, $[NO_3]^-$	N/A	N/A	12
3	$[Bi(TeO_3)](NO_3)$	*P*2$_1$/*c*	$[TeO_3]^{2-}$, $[NO_3]^-$	3.62	N/A	13
4	$Bi_3(\mu_3\text{-}OH)(TeO_3)_3(NO_3)_2$	*P*-62*m*	$[Te_3O_{10}]^{8-}$, $[NO_3]^-$	3.31	N/A	14
5	$La(TeO_3)(NO_3)$	*P*2$_1$/*n*	$[TeO_3]^{2-}$, $[NO_3]^-$	3.7	N/A	15
6	$Nd(TeO_3)(NO_3)$	*P*2$_1$/*n*	$[TeO_3]^{2-}$, $[NO_3]^-$	3.6	N/A	15
7	$Eu(TeO_3)(NO_3)$	*Cmca*	$[TeO_4]^{4-}$, $[NO_3]^-$	3.7	N/A	15
8	$Gd(TeO_3)(NO_3)$	*Cmca*	$[TeO_4]^{4-}$, $[NO_3]^-$	3.8	N/A	15
9	$Dy(TeO_3)(NO_3)$	*Cmca*	$[TeO_4]^{4-}$, $[NO_3]^-$	3.8	N/A	15
10	$Er(TeO_3)(NO_3)$	*Cmca*	$[TeO_4]^{4-}$, $[NO_3]^-$	3.8	N/A	15
11	$Y(TeO_3)(NO_3)$	*Cmca*	$[TeO_4]^{4-}$, $[NO_3]^-$	4.4	N/A	15
12	$(SbTeO_3)(NO_3)$	*Pca*2$_1$	$[TeO_3]^{2-}$, $[NO_3]^-$	4.32	0.081@546nm	16

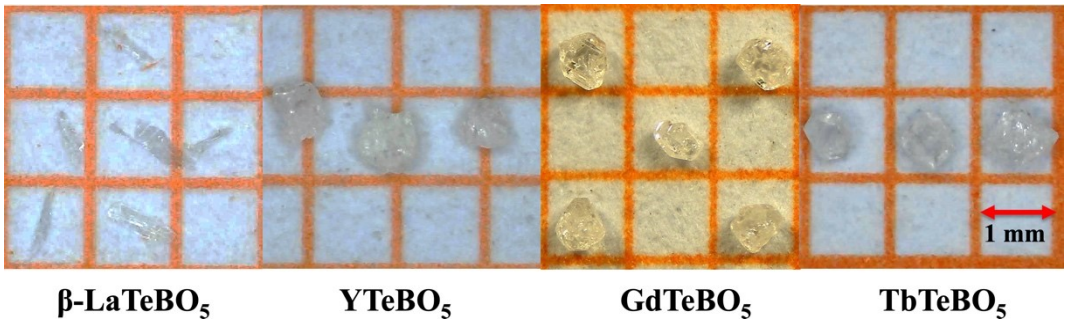

Figure S1. The photographs of crystals for β-$LaTeBO_5$ and $RETeBO_5$ (RE = Y, Gd, Tb).

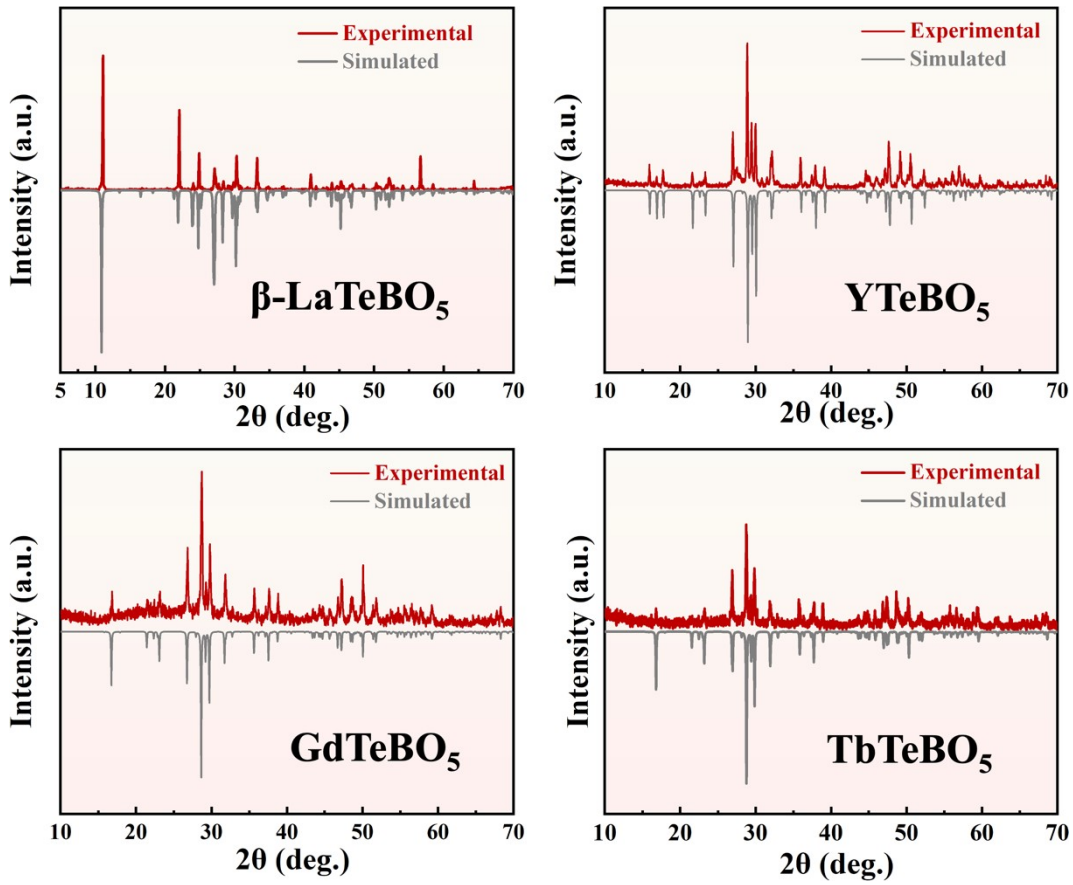

Figure S2. Simulated and experimental powder X-ray diffraction patterns of β-$LaTeBO_5$ and $RETeBO_5$ (RE = Y, Gd, Tb) in room temperature.

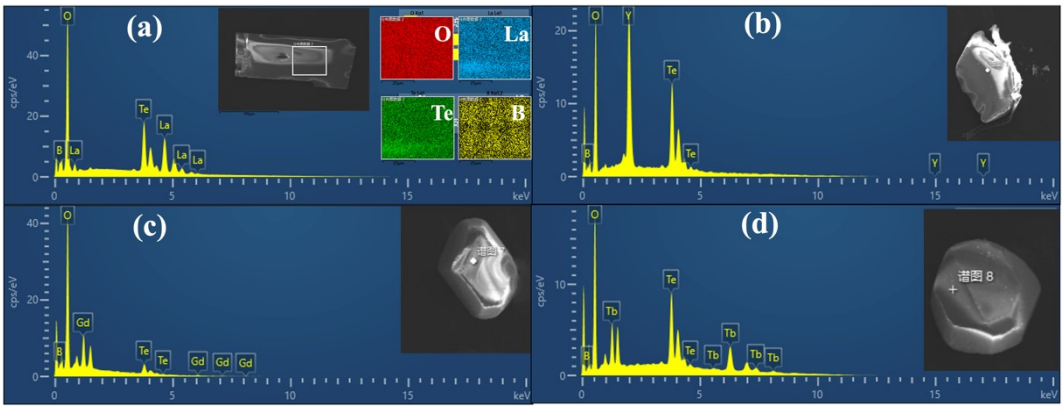

Figure S3. EDS spectrum of β-$LaTeBO_5$ (a) and $RETeBO_5$ (RE = Y (b), Gd (c), Tb (d)).

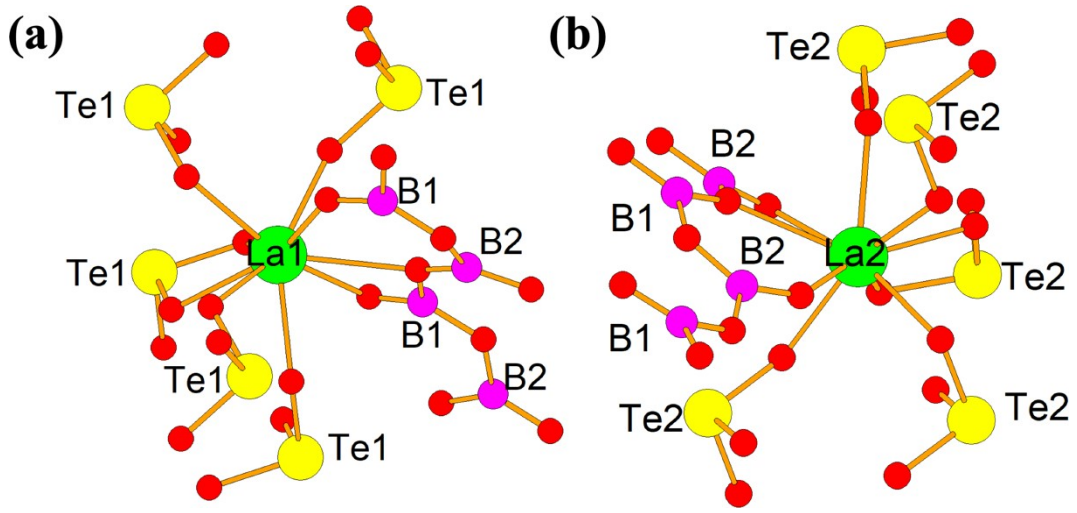

Figure S4. The coordination environment around La (1) atom (a) and La (2) atom (b) in β-$LaTeBO_5$.

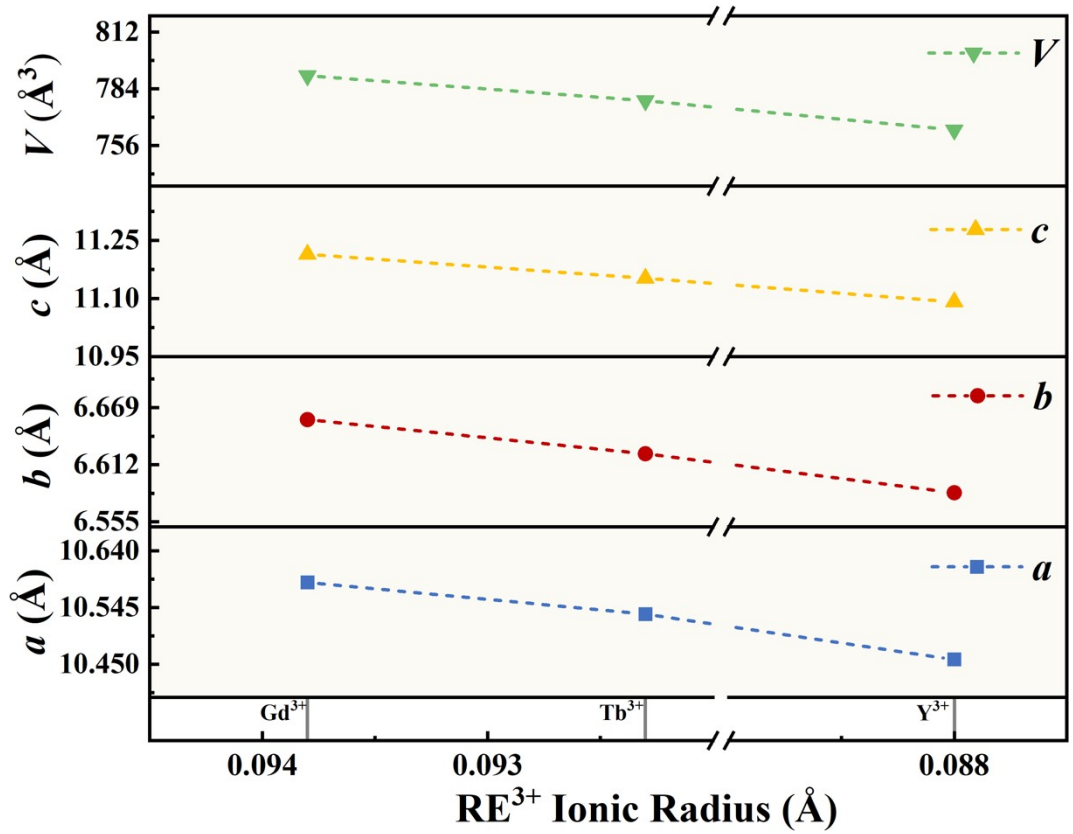

Figure S5. Plot of lattice constant (which contains the *a*, *b*, *c* and *V*) for $RETeBO_5$ (RE = Y, Gd, Tb) against the RE^{3+} ionic radius.

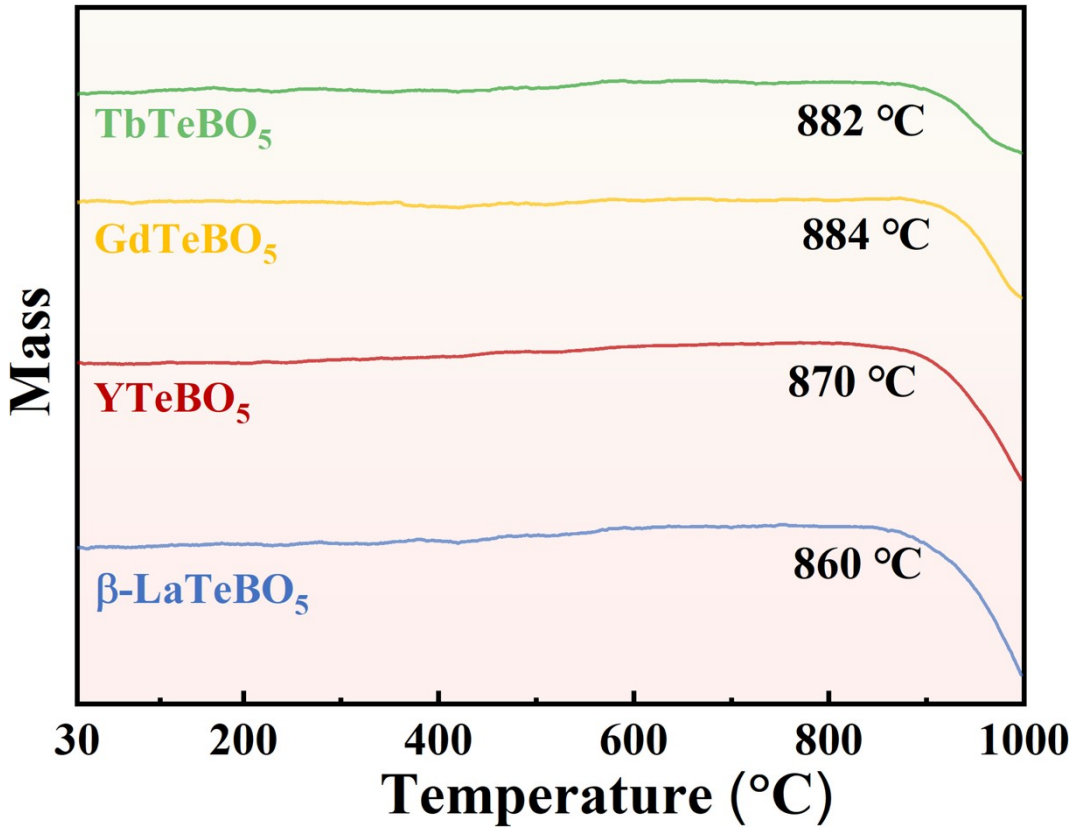

Figure S6. TG curves of β-$LaTeBO_5$ and $RETeBO_5$ (RE = Y, Gd, Tb).

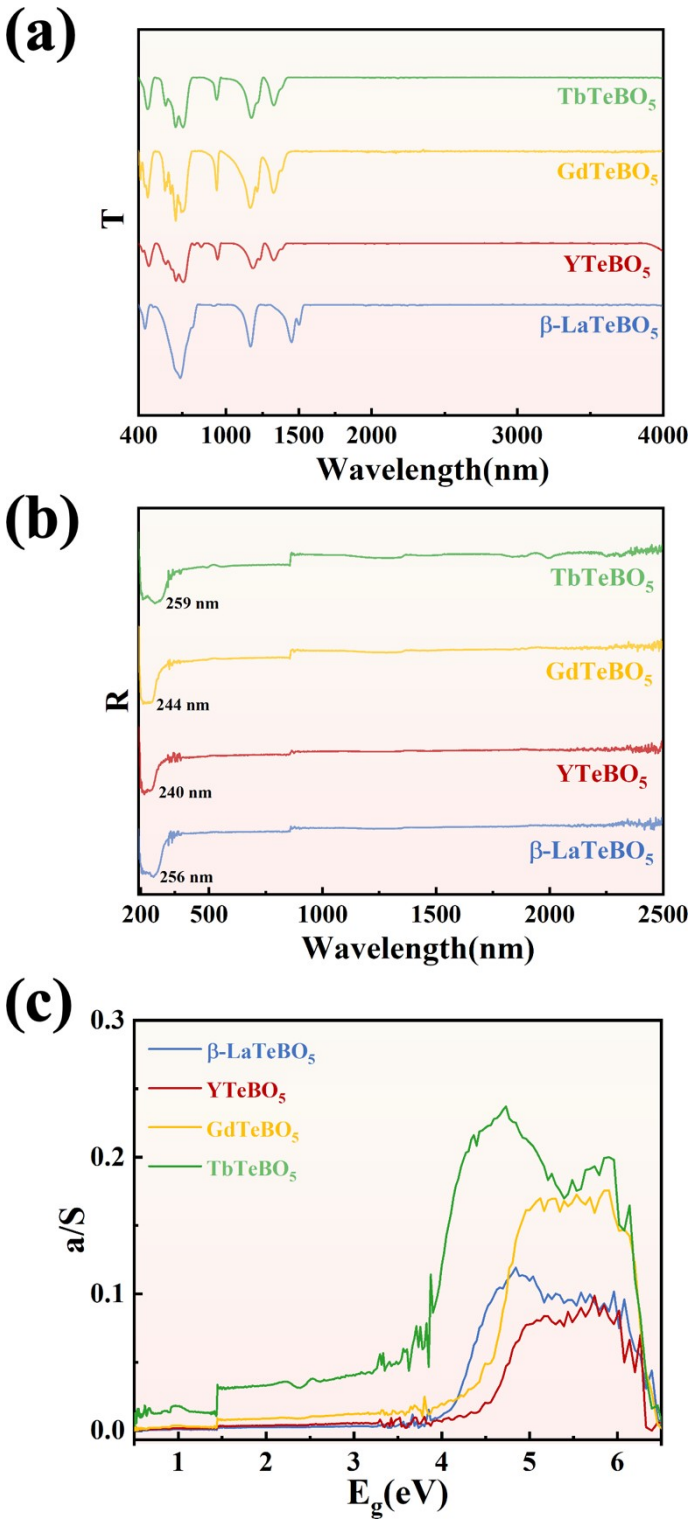

Figure S7. Spectrum of β-$LaTeBO_5$ and $RETeBO_5$ (RE = Y, Gd, Tb): (a) IR spectrum; (b) UV-vis-NIR diffuse reflectance spectrum; (c) Converted F(R)-versus-Energy plot.

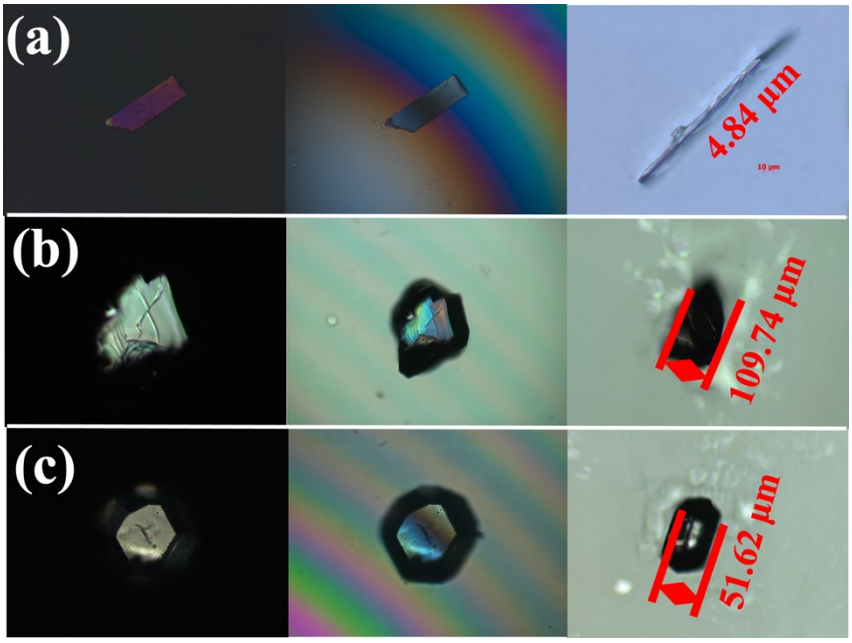

Figure S8. The positive and negative rotation of compensatory, and the thickness of β-$LaTeBO_5$ (a), $YTeBO_5$ (b) and $GdTeBO_5$ (c).

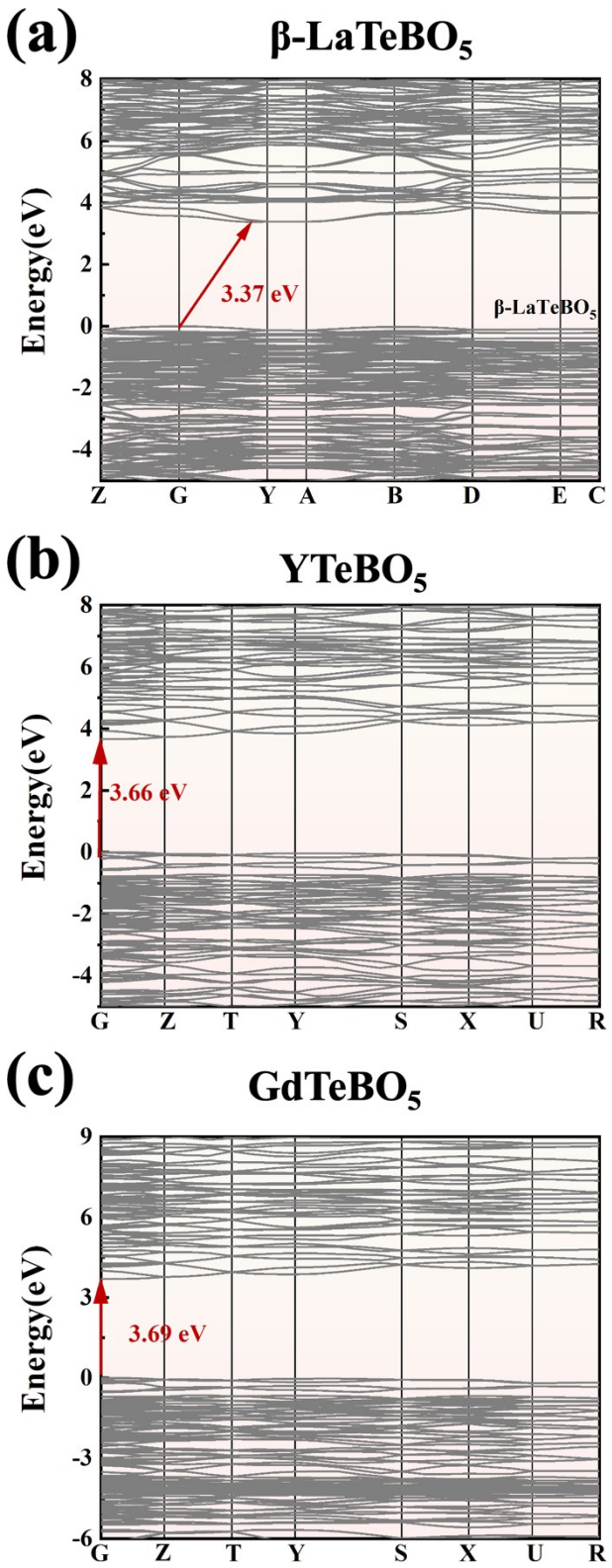

Figure S9. The calculated band structure of β-$LaTeBO_5$ (a) and $RETeBO_5$ (RE = Y(b), Gd(c)).

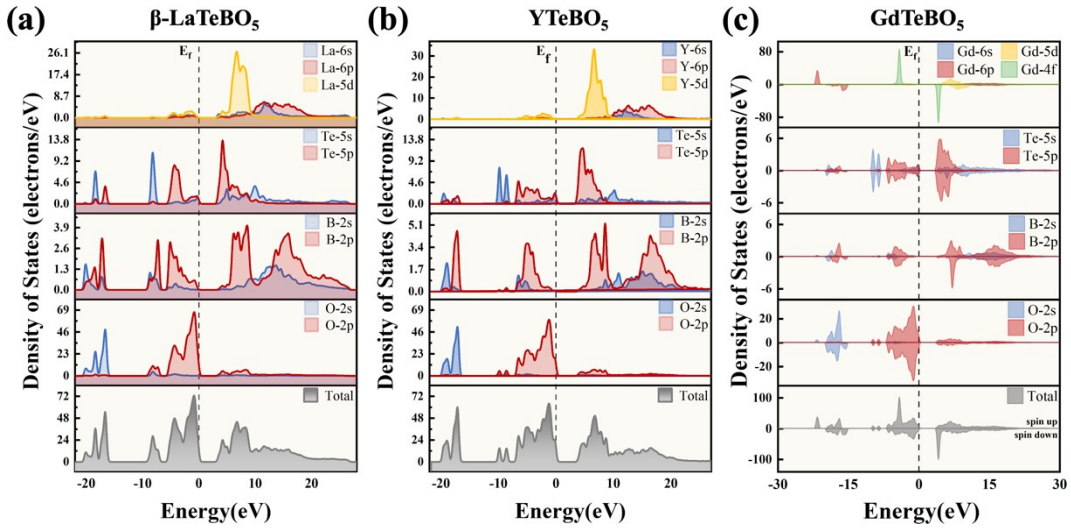

Figure S10. Total and partial density of states of β-$LaTeBO_5$ (a) and $RETeBO_5$ (RE = Y(b), Gd(c)).

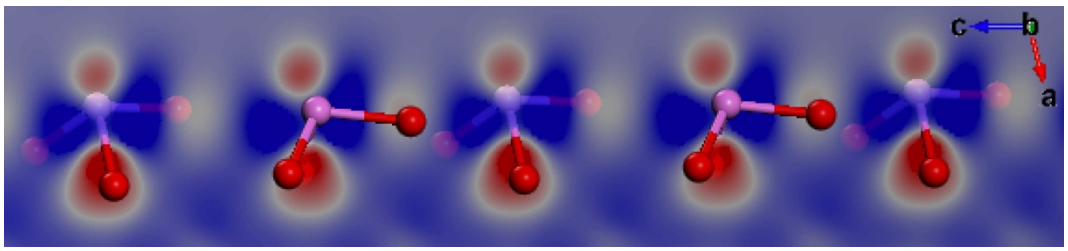

Figure S11. Electron density difference maps of $[TeO_3]^{2-}$ units in β-$LaTeBO_5$ along the *b* axis.

References

1. M. Weil, G. Heymann and H. Huppertz, The High-Pressure Polymorph of $Ca_4Te_5O_{14}$ and the Mixed-Valent Compound $Ca_{13}Te^{VI}_{2/3}Te^{IV}_{3.75}O_{15}(BO_3)_4(OH)_3$, *Eur. J. Inorg. Chem.*, 2016, **2016**, 3574-3579.
2. J. Sun, M. Mutailipu, S. Cheng, Z. Yang and S. Pan, $Rb_3BaTeB_7O_{15}$: a novel $[B_7O_{16}]$ fundamental building block in a new telluroborate with $[TeO_3]$ polyhedra, *Dalton Trans.*, 2020, **49**, 8911-8917.
3. T. Zhang, L.-H. Deng, W.-L. Xie, C.-Y. Bai, J.-W. Feng, J.-J. Zheng and D.-H. An, $K_3BaTeB_7O_{15}$: A new borotellurite with mixed metal cations, *J. Mol. Struct.*, 2022, **1252**, 132181.
4. R. Zhang, A. Tudi, X. Yang, X. Wang, Z. Yang, S. Han and S. Pan, $PbTeB_4O_9$: a lead tellurium borate with unprecedented fundamental building block $[B_4O_{10}]$ and large birefringence, *Chem. Commun.* , 2024, **60**, 340-343.
5. R. Ziegler, G. Heymann and H. Huppertz, Synthesis and crystal structure of the first ternary tellurium borate TeB_4O_8, *Z. Anorg. Allg. Chem.*, 2022, **648**, e202200229.
6. R. Ziegler, F. R. S. Purtscher, T. S. Hofer, G. Heymann and H. Huppertz, Single-crystal structure and theoretical calculations of the second ternary tellurium borate $Te_2B_2O_7$, *J. Solid State Chem.*, 2024, **330**, 124458.
7. J. Wang, H. Wu, H. Yu, Z. Hu, J. Wang and Y. Wu, $LaTeBO_5$: a new borotellurite with a large birefringence activated by the highly distorted $[Te^{(iv)}O_4]$ group, *Dalton Trans.*, 2021, **50**, 12404-12407.
8. R. Fischer, F. Pertlik and J. Zemann, The crystal structure of mroseite, $CaTeO_2(CO_3)$, *Can. Mineral.*, 1975, **13**, 383-387.
9. F. Eder, B. Stöger and M. Weil, Order-disorder (OD) structures of $Rb_2Zn(TeO_3)(CO_3)\cdot H_2O$ and $Na_2Zn_2Te_4O_{11}$, *Z. Kristallogr.*, 2022, **237**, 329-341.
10. P. F. Chen, C. L. Hu, M. Y. Cao, X. Y. Zhang and J. G. Mao, $AKTeO_2(CO_3)$ (A = Li, Na): The First Carbonatotellurites Featuring a Zero-Dimensional $[Te_2C_2O_{10}]^{4-}$ Cluster and a Wide Band Gap, *Inorg. Chem.*, 2023, **62**, 6864-6870.
11. S. Lee, H. Jo and K. M. Ok, $Bi_2Te_2O_6(NO_3)_2(OH)_2(H_2O)$: A layered bismuth tellurium nitrate hydroxide with multiple noncentrosymmetric chromophores, *J. Solid State Chem.*, 2019, **271**, 298-302.
12. C. Olsson, L.-G. Johansson and S. Kazikowski., Structure of Silver Telluryl Nitrate, $AgTeO_2NO_3$, *Acta Cryst.*, 1988, **C44**, 427-429.
13. C.-Y. Meng, M.-F. Wei, L. Geng, P.-Q. Hu, M.-X. Yu and W.-D. Cheng, Synthesis, structure, and characterization of two new bismuth(III) selenite/tellurite nitrates: $[(Bi_3O_2)(SeO_3)_2](NO_3)$ and $[Bi(TeO_3)](NO_3)$, *J. Solid State Chem.*, 2016, **239**, 46-52.
14. J. L. Song and C. Qian, Syntheses, Crystal Structures, and Properties of Two Quaternary Selenite/Tellurite-Nitrates with Formula of $Bi(SeO_3)(NO_3)$ and $Bi_3(\mu_3\text{-}OH)(TeO_3)_3(NO_3)_2$, *ChemistrySelect*, 2017, **2**, 1681-1685.
15. H. E. Lee, H. Jo, M. H. Lee and K. M. Ok, Unique synthesis, structure determination, and optical properties of seven new layered rare earth tellurite nitrates, $RE(TeO_3)(NO_3)$ (RE = La, Nd, Eu, Gd, Dy, Er, and Y), *J. Alloys Compd.*, 2021, **851**, 156855.
16. B. Zhang, C. L. Hu, J. G. Mao and F. Kong, Fully tricoordinated assembly unveils a pioneering nonlinear optical crystal $(SbTeO_3)(NO_3)$, *Chem. Sci.*, 2024, **15**, 18549-18556